Journal of Power Sources 194 (2009) 574–579

Contents lists available at ScienceDirect

Journal of Power Sources

journal homepage: www.elsevier.com/locate/jpowsour

Short communication

Nanostructured photoelectrode consisting of TiO_2 hollow spheres for non-volatile electrolyte-based dye-sensitized solar cells

Jong Hyuk Park[a], Sun Young Jung[b], Raehyun Kim[a], Nam-Gyu Park[c], Junkyung Kim[a], Sang-Soo Lee[a,*]

[a] Hybrid Materials Research Center, Korea Institute of Science and Technology, Seoul 136-791, Republic of Korea
[b] Department of Chemical and Biological Engineering, Korea University, Seoul 136-701, Republic of Korea
[c] Solar Cell Research Center, Korea Institute of Science and Technology, Seoul 136-791, Republic of Korea

ARTICLE INFO

Article history:
Received 10 January 2009
Received in revised form 18 March 2009
Accepted 30 March 2009
Available online 18 April 2009

Keywords:
Dye-sensitized solar cell
Hollow sphere
Non-volatile electrolyte
Light-harvesting
Electron diffusion

ABSTRACT

A photoelectrode consisting of titania hollow spheres for dye-sensitized solar cells (DSSCs) is prepared by a paste method and the effect of the nanostructure on the performance of DSSCs with non-volatile electrolytes is investigated. The structure of the hollow sphere (HS) electrode with a large pore size and a high porosity allows highly viscous non-volatile electrolytes to penetrate the electrode thoroughly. Furthermore, its outstanding light-harvesting efficiency and long electron diffusion length make the efficiency of the DSSCs with the HS electrode comparable with those of a conventional nanocrystalline electrode, in spite of the smaller amount of the adsorbed dye, when oligomer electrolytes are used. The results show that the structure of a photoelectrode highly improves the performance of the device and the HS electrode is an effective structure for the use of non-volatile electrolytes in DSSCs.

1. Introduction

In the past two decades, the dye-sensitized solar cell (DSSC) has drawn much interest owing to its low production cost and thereby its capability to replace conventional solar cells [1–11]. Extensive research on each component of DSSCs, including sensitizers [3–5], electrodes [6–8], and electrolytes [9,10] has been performed to enhance their performance and, as a result, an energy-conversion efficiency of over 11% has been demonstrated [11]. For the practical application of DSSCs, long-term stability, as well as high efficiency, is required. Nevertheless, volatile solvent electrolytes that are commonly used in DSSCs with a high efficiency have a restriction on guaranteeing the stability due to the evaporation or leakage of solvent. While stable non-volatile electrolytes such as ionic liquids [12,13], oligomers [14,15] conducting polymers [16] and hole conductors [17] have been examined as alternatives to a volatile solvent, employing these materials to DSSCs is limited in terms of efficiency compared with the use of volatile solvent electrolytes. One of the possible reasons for this drawback could be the structure of photoelectrodes that generally is not suitable for highly viscous, non-volatile electrolytes to penetrate the nanopores in photoelectrodes. Accordingly, it is possible that the electrodes with a structure suitable for non-volatile electrolytes may considerably improve the performance of DSSCs. Recently, the novel structures of a photoelectrode have been reported through the use of nanowires [18,19], nanotubes [20,21], and hollow spheres [22,23]. In particular, electrodes containing a hollow structure have shown significant potential to yield an outstanding light-harvesting efficiency [22,23]. Moreover, the hollow structure of the electrodes would have an additional advantage in that the large porosity would provide good permeability for non-volatile electrolytes with high viscosity. Low area density and significant defects such as cracks, however, prevent the hollow structure electrodes from exhibiting a performance comparable with that of conventional nanocrystalline (NC) electrodes [22].

This study reports the preparation of electrodes consisting of TiO_2 hollow spheres (HS electrodes) by means of a paste method. The HS electrode shows high area density and desirable thickness without cracks. Application of the HS electrode to DSSCs with non-volatile electrolytes yields superior light-harvesting efficiency and long electron diffusion length. To the best of our knowledge, this is the first demonstration that the structure of HS electrodes improves the efficiency of DSSCs with non-volatile electrolytes.

2. Experimental

2.1. Preparation of TiO_2 hollow spheres

For the preparation of the polymer templates for hollow spheres, 110 g of purified styrene was added to 1000 g of deionized water

* Corresponding author. Tel.: +82 2 958 5356; fax: +82 2 958 5309.
E-mail address: s-slee@kist.re.kr (S.-S. Lee).

0378-7753/$ – see front matter © 2009 Elsevier B.V. All rights reserved.
doi:10.1016/j.jpowsour.2009.03.075

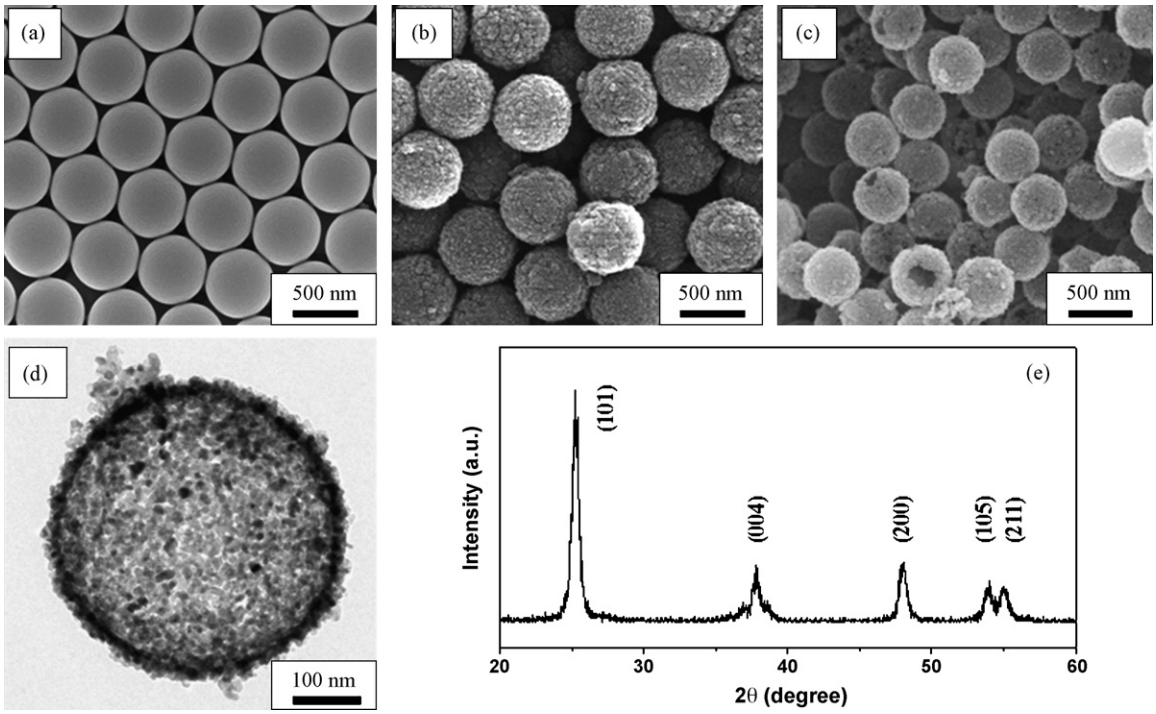

Fig. 1. SEM images of (a) synthesized PS, (b) TiO_2-coated PS and (c) TiO_2 hollow spheres, (d) TEM image and (e) XRD pattern of TiO_2 hollow spheres.

and mechanically stirred at 350 rpm under a nitrogen atmosphere. The temperature of the solution was maintained at 70 °C. Polymerization was initiated by adding 0.5 g of ammonium persulfate [24]. After 30 h of polymerization, the reaction was stopped by rapid quenching and the residual monomer was removed through dialysis using cellulose tubular membranes (Membrane Filtration Products, T2). To construct a TiO_2 shell on the polystyrene (PS) sphere, 25 g of the aqueous solution containing the prepared PS spheres (3.5 wt%) was mixed with 125 g of 0.2 M titanium chloride solution and stirred at 53 °C for 90 min. The product was repeatedly washed by centrifuging and coated again by the same method to increase the shell thickness. After freeze-drying, the TiO_2-coated particles were sintered at 500 °C for 30 min at a heating rate of 5 °C min^{-1} to remove the PS template and form a hollow structure.

2.2. Fabrication of DSSCs

A paste for the fabrication of the HS electrode was prepared by mixing TiO_2 hollow spheres with terpineol, ethyl cellulose, lauric acid and ethanol, and then evaporating of ethanol [23]. Commercial TiO_2 paste (18NR-T, STI) was used for the NC electrode. The fabrication methods of the photo and counter electrodes have been described previously [25–27]. Ti(IV) bis(ethyl acetoacetato)-diisopropoxide solution was spincoated on transparent fluorine-doped tin oxide glass (Pilkington, TEC-8, 8 Ω sq^{-1}) and annealed at 500 °C for 15 min to form a blocking layer. To control the thickness of the photoelectrodes, the substrates were covered on two parallel edges with tape. The paste for each electrode was cast on the blocking layer using a doctor blade and heated sequentially at 150 °C for 30 min and at 500 °C for 15 min. The sintered electrodes were immersed in ethanol containing 0.5 mM of purified dye (N719, Solaronix) for 24 h. A platinum layer on the counter electrodes was fabricated by spincoating H_2PtCl_6 solution and then heating at 400 °C for 20 min. The photo and the counter electrodes were sealed with a thermal adhesive film of thickness 25 μm, and then filled with an oligomer electrolyte of poly(ethylene glycol dimethyl ether) (molecular weight = 250 g mol^{-1}) containing 0.8 M 1-butyl-3-methylimidazolium iodide, 0.1 M iodine and 0.1 M N-methylbenzimidazole.

2.3. Characterization

Scanning electron microscopy (SEM) (FEI, Nova 200 NanoSEM) and transmission electron microscopy (TEM) (Philips, CM30) were used to observe the morphology of the spheres and electrodes. The crystallinity of the TiO_2 hollow spheres was investigated by means of X-ray diffraction (XRD) (Rigaku, D/MAX-2500). The thickness of the electrodes was obtained by using a surface profiler (KLA-Tencor, Alpha-Step IQ). The pore-size distribution of the hollow structure and the nanocrystalline electrode was obtained by Brunauer–Emmett–Teller (BET) measurements (Bel Japan, Belsorp-max) and the reflectance of each electrode was detected using a UV–vis spectrometer (Jasco, V-670) with an integrating sphere. The electron diffusion coefficient, lifetime and diffusion length in each electrode were estimated by stepped light-induced transient measurements of photocurrent and voltage [28,29]. A diode laser with a wavelength of 635 nm was operated at a voltage of 3.00 V and stepped down to 2.90 V. The laser intensity was varied by using ND filters. *J–V* curves of the prepared DSSCs were measured under AM 1.5 G illumination (100 mW cm^{-2}). The active areas were in the range of 0.26 ± 0.01 cm^2 for all of the cells. Incident-photon-to-current conversion efficiency (IPCE) data from 400 to 800 nm were obtained using a specially designed IPCE system for DSSCs (PV Measurements Inc.) [23]. To measure the amount of adsorbed dye on the photoelectrodes, the sensitizer was desorbed using a 0.1 M NaOH solution in water and ethanol (50:50, v/v) and absorption spectra of the solution were detected by a UV–vis spectrometer [23].

3. Results and discussion

3.1. TiO_2 hollow spheres

Hollow spheres are generally prepared by coating polymer templates with metal or inorganic materials and then eliminating the

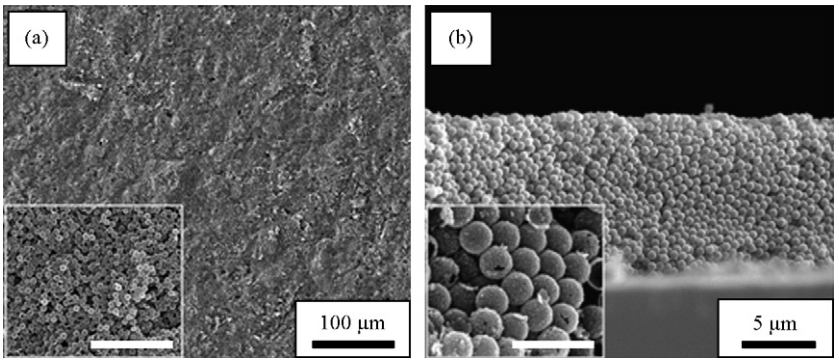

Fig. 2. SEM images of HS electrode: (a) top and (b) cross-sectional view of electrode. White scale bars of inlet at (a) and (b) represent 5 and 1 μm, respectively.

templates [30,31]. Considering the light scattering effect and surface area of the photoelectrode in DSSCs, the diameter of hollow spheres is controlled to the submicron level, especially in the range of 400–500 nm. Emulsion polymerization is frequently used to fabricate submicron polymer spheres in order to obtain spherical, size-controlled and monodispersed particles [32]. A SEM image of PS spheres prepared by emulsifier-free emulsion polymerization is shown in Fig. 1(a). Hexagonal packing of the PS spheres confirms that the PS particles are monodispersed and their size is approximately 540 nm. Negative surface charge, originated from an anionic initiator (ammonium persulfate) in the emulsion polymerization, helps the TiO_2 nanoparticles to adsorb easily on the surface of the PS particles [31,33]. Coating TiO_2 nanoparticles on the surface of the PS spheres was conducted by a simple method, i.e., mixing and stirring PS spheres with $TiCl_4$ solution while heating, that enables the preparation of a large amount of coated particles. The spheres were coated twice to ensure maintenance of the hollow structure before removing the templates (Fig. 1(b)). The coated particles were sintered at 500 °C for 30 min to remove the PS template and also to improve the crystallinity and the connectivity of TiO_2 particles. Analysis by SEM and TEM (Fig. 1(c) and (d)) confirm that the TiO_2 hollow spheres are well constructed and the diameter and the shell thickness are approximately 430 and 30 nm, respectively. An XRD pattern of the TiO_2 hollow spheres is presented in Fig. 1(e). It shows that the crystalline phase is an entirely anatase form and the crystalline size is estimated as 15.1 nm from the Scherer equation [23].

3.2. Photoelectrode consisting of TiO_2 hollow spheres

A paste containing the hollow spheres was prepared for the fabrication of the HS electrodes. As reported previously [22], a desirable morphology of the HS electrode is difficult to prepare. By contrast, the paste method used here provides crack-free electrodes with high area density and suitable thickness, and also enhances the connectivity between the spheres. Ethyl cellulose was selected as a binder to improve the connectivity between the TiO_2 hollow spheres. The amount of a medium such as terpineol was adjusted to control the viscosity of the paste and the thickness of the electrodes. Lauric acid was added to the paste to reduce aggregation between the spheres. The paste was cast on to transparent conducting oxide substrates that had been pre-coated with a blocking layer, which plays a significant role in improving the interconnectivity between the HS electrode and the substrate and prevents electron recombination [34]. After applying the paste with a doctor blade, HS electrodes were constructed by annealing. Fig. 2(a) and (b) illustrates the morphology of the HS electrodes made by the paste method. It is seen to be crack-free and has a desirable thickness (12 ± 0.5 μm).

The pore-size distribution and surface area of the HS and NC electrodes were determined from BET measurements. The HS electrode has large pores (peak: 51.8 nm), more so than the NC electrode (peak: 14.0 nm), while the surface area of the former ($61.9\ m^2\ g^{-1}$) is smaller than that of the latter ($90.9\ m^2\ g^{-1}$) (Fig. 3). For electrodes with a similar thickness, the area density of the HS electrode is lower ($0.84\ mg\ cm^{-2}$) than that of the NC electrode ($1.65\ mg\ cm^{-2}$). Accordingly, it can be expected that the overall pore volume in the HS electrode is larger than in the NC electrode. The larger pore volume will allow non-volatile electrolytes with high viscosity to penetrate more easily into the HS electrode. As shown in the UV–vis reflectance spectra for each electrode with and without N719 dye adsorption (Fig. 4), the HS electrode exhibits much higher reflectance than the NC electrode. Although the reflectance decreases significantly in the range of 400–600 nm after dye adsorption, the HS electrode still has large reflectance at long wavelengths (over 600 nm) (Fig. 4(b)). The former is supposed to scatter light better than the latter. The scattered light appears to increase the amount of electrons generated in the photoelectrode.

3.3. Photovoltaic performance

The HS and NC electrodes were applied to DSSCs that contained an oligomer [poly(ethylene glycol dimethyl ether), molecular weight = $250\ g\ mol^{-1}$] electrolyte. The performance is listed in Table 1. The energy-conversion efficiency of the DSSCs with the HS electrode was 4.30%, which is about 87% of that with the NC electrode (4.95%). This difference mainly originates from the short-circuit current density (J_{SC}). The current density of the DSSCs with NC electrodes is $11.90\ mA\ cm^{-2}$ while that of the DSSCs with HS electrodes is only $8.62\ mA\ cm^{-2}$. However, considering the amount of the dye adsorbed on the HS electrode ($0.343 \times 10^{-7}\ mol\ cm^{-2}$) compared with that of the NC electrode ($1.104 \times 10^{-7}\ mol\ cm^{-2}$), it is concluded that the current density is enhanced by using the HS electrode. Fig. 5 exhibits the IPCE spectra of the DSSCs with HS

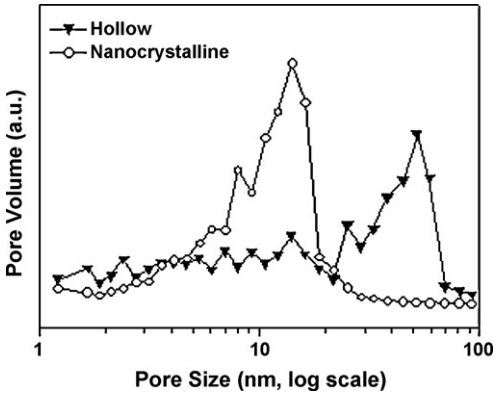

Fig. 3. Pore-size distribution of HS and NC electrodes.

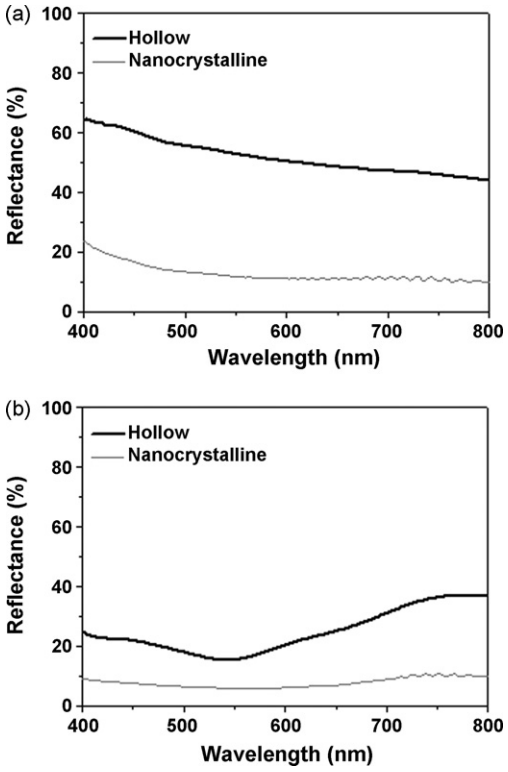

Fig. 4. Diffused reflectance spectra of HS and NC electrodes (a) without and (b) with adsorption of N719 dye.

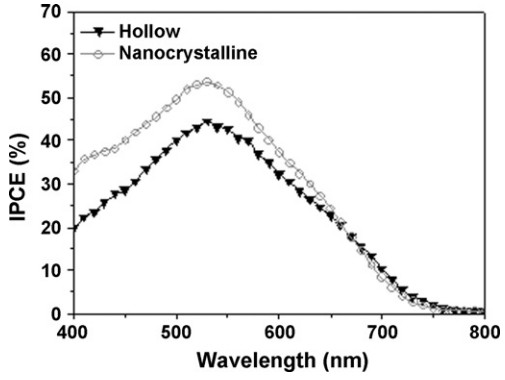

Fig. 5. IPCE spectra of DSSCs based on HS and NC electrodes.

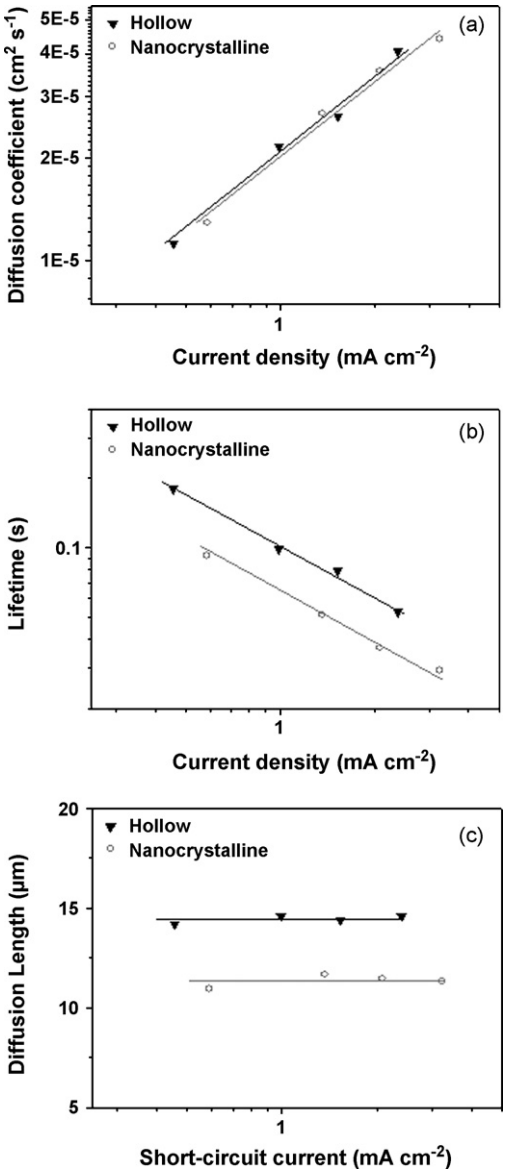

Fig. 6. Electron (a) diffusion coefficient, (b) lifetime and (c) diffusion length in HS and NC electrodes of DSSCs with oligomer electrolytes. Thickness of each electrode controlled in the range of 7–9 μm.

and NC electrodes. The IPCE data also suggest that the HS electrode increases the current density. Although the amount of adsorbed dye in the HS electrode is one-third of that in the NC electrode, the IPCE value of the HS electrode is comparable with that of the NC electrode at over 650 nm. Therefore, it can be expected that one of the reasons for the relatively high current density of the HS electrode is its light-scattering effect in the long wavelength region.

Another possible reason for the high current density is the electron lifetime in HS electrodes. The higher open-circuit voltage (V_{OC}) and fill factor (FF) of the DSSCs employing the HS electrode suggest that the recombination between the electrons in the HS electrode and I_3^- ions in the electrolytes is suppressed due to the smaller surface area of the HS electrode compared with that of the NC electrode. To obtain the electron lifetime directly, transient measurements of photocurrent and voltage were conducted. Reliable data are obtained only when the thickness of the photoelectrodes is thinner than the electron diffusion length. Therefore, the thickness of the electrodes for transient measurements was controlled in the range of 7–9 μm. Although the thickness of the electrodes is not equal to that of the cells used at *J–V* measurements, the electron transport properties will not be largely changed by the

Table 1
Properties of HS and NC electrodes and performance of DSSCs employing each electrode.

Samples	Thickness [μm]	Area density [mg cm^{-2}]	Adsorbed dye [$\times 10^{-7}$ mol cm^{-2}][a]	V_{OC} [V]	J_{SC} [mA cm^{-2}]	FF	η [%]
Hollow	12.0 ± 0.5	0.84	0.343	0.720	8.62	0.691	4.30
Nanocrystalline	12.1 ± 0.1	1.65	1.104	0.703	11.90	0.592	4.95

[a] Amount of adsorbed dye is divided by active area not volume because value per unit area has much correlation with the area density.

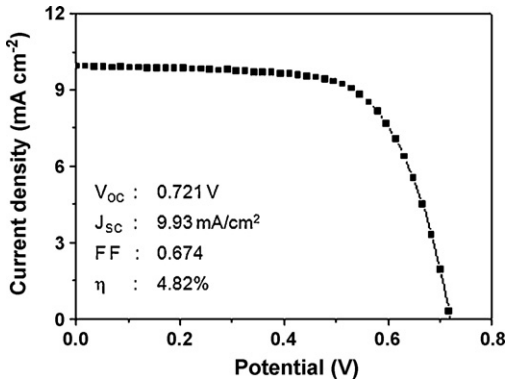

Fig. 7. *J–V* curve of DSSC containing HS electrode with oligomer electrolytes. Thickness of HS electrode is about 16.0 μm.

electrode thickness. While there is no significant difference in the electron diffusion coefficient, HS electrodes have longer electron lifetime than NC electrodes (Fig. 6(a) and (b)). This brings longer electron diffusion length in the former (~14.5 μm) than the latter (~11.0 μm) (Fig. 6(c)). The longer electron diffusion length of the HS electrode implies that its small surface area and amount of adsorbed dye can be improved by increasing the electrode thickness. While the electrode with a thickness of over 12 μm does not result in an increase of the cell efficiency in the case of NC electrodes due to their short electron diffusion length (the data are not shown here), the maximum efficiency is produced when the thickness of the HS electrode is about 16.0 μm. The *J–V* curve of a DSSC with a HS electrode of thickness 16.0 μm is given in Fig. 7. The J_{SC} increases to 9.93 mA cm^{-2} without a considerable decrease of V_{OC} and FF compared with the data of the thinner HS electrode (Table 1). In addition, the cell efficiency is almost identical to that of a cell with a NC electrode.

Using volatile electrolytes, a relatively large efficiency difference between HS and NC electrodes is observed (Fig. 8), while the HS electrode with optimized thickness shows an efficiency equal to that of the NC electrode when oligomer electrolytes are used. This suggests that the structure of the electrodes influences permeation of the electrolytes. In other words, penetration of the oligomer electrolyte with poor permeability is facilitated by the HS electrode in contrast to the NC electrode. The high porosity of the HS electrode benefits the use of viscous electrolytes and ultimately improves the performance of DSSCs that employ oligomer electrolytes.

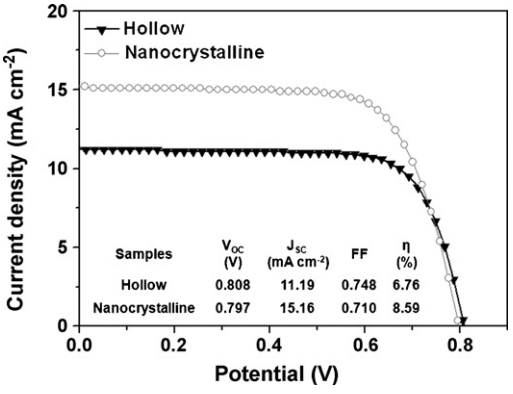

Fig. 8. *J–V* curves of DSSC with HS and NC electrodes employing a volatile solvent electrolyte. Volatile solvent electrolyte is comprised of 0.7 M 1-butyl-3-methylimidazolium iodide, 0.03 M iodine, 0.5 M tert-butylpyridine and 0.1 M guanidine thiocyanate in acetonitrile/valeronitrile (v/v = 85/15) solution. Thicknesses of HS and NC electrodes are about 16.0 and 12.1 μm, respectively.

4. Conclusions

HS electrodes have been introduced into DSSCs employing oligomer electrolytes and the effect of the electrode structure on the cell performance has been investigated. The paste method is useful to fabricate HS electrodes with a high area density, desirable thickness and no cracks. It is found that the large pore size and the high porosity of the HS electrode benefit penetration of the oligomer electrolyte. Moreover, the outstanding light-harvesting efficiency and long electron diffusion length of the HS electrode elevate its current density and thereby compensate for its small amount of adsorbed dye. These effects result in the efficiency of DSSCs with the HS electrode being comparable with that of a NC electrode when oligomer electrolytes are employed. Consequently, HS electrodes will be a promising means to improve the performance of DSSCs containing other non-volatile electrolytes as well as oligomer electrolytes.

Acknowledgements

This work was supported by the KIST internal project under contract 2E20980. We thank Prof. Yong Soo Kang at Hanyang University for the use of the transient measurements of photocurrent and voltage and Dr. Hyunjung Lee at KIST for helpful discussions.

References

[1] B. O'Regan, M. Grätzel, Nature 353 (1991) 737–740.
[2] M. Grätzel, Nature 414 (2001) 338–344.
[3] M.K. Nazeeruddin, A. Kay, I. Rodicio, R. Humphry-Baker, E. Müller, P. Liska, N. Vlachopoulos, M. Grätzel, J. Am. Chem. Soc. 115 (1993) 6382–6390.
[4] M.K. Nazeeruddin, P. Péchy, T. Renouard, S.M. Zakeeruddin, R. Humphry-Baker, P. Comte, P. Liska, L. Cevey, E. Costa, V. Shklover, L. Spiccia, G.B. Deacon, C.A. Bignozzi, M. Grätzel, J. Am. Chem. Soc. 123 (2001) 1613–1624.
[5] N. Robertson, Angew. Chem. Int. Ed. 45 (2006) 2338–2345.
[6] A.J. Frank, N. Kopidakis, J. van de Lagemaat, Coord. Chem. Rev. 248 (2004) 1165–1179.
[7] J.R. Durrant, S.A. Haque, E. Palomares, Coord. Chem. Rev. 248 (2004) 1247–1257.
[8] M. Quintana, T. Edvinsson, A. Hagfeldt, G. Boschloo, J. Phys. Chem. C 111 (2007) 1035–1041.
[9] B.A. Gregg, Coord. Chem. Rev. 248 (2004) 1215–1224.
[10] A.F. Nogueira, C. Longo, M.-A. De Paoli, Coord. Chem. Rev. 248 (2004) 1455–1468.
[11] M. Grätzel, J. Photochem. Photobiol. A: Chem. 164 (2004) 3–14.
[12] P. Wang, S.M. Zakeeruddin, P. Comte, I. Exnar, M. Grätzel, J. Am. Chem. Soc. 125 (2003) 1166–1167.
[13] D. Kuang, P. Wang, S. Ito, S.M. Zakeeruddin, M. Grätzel, J. Am. Chem. Soc. 128 (2006) 7732–7733.
[14] Y.J. Kim, J.H. Kim, M.-S. Kang, M.J. Lee, J. Won, J.C. Lee, Y.S. Kang, Adv. Mater. 16 (2004) 1753–1757.
[15] J.H. Kim, M.-S. Kang, Y.J. Kim, J. Won, N.-G. Park, Y.S. Kang, Chem. Commun. (2004) 1662–1663.
[16] Y. Saito, T. Azechi, T. Kitamura, Y. Hasegawa, Y. Wada, S. Yanagida, Coord. Chem. Rev. 248 (2004) 1469–1478.
[17] U. Bach, D. Lupo, P. Comte, J.E. Moser, F. Weissörtel, J. Salbeck, H. Spreitzer, M. Grätzel, Nature 395 (1998) 583–585.
[18] J.B. Baxter, E.S. Aydil, Appl. Phys. Lett. 86 (2005) 053114.
[19] M. Law, L.E. Greene, J.C. Johnson, R. Saykally, P.D. Yang, Nat. Mater. 4 (2005) 455–459.
[20] G.K. Mor, K. Shankar, M. Paulose, O.K. Varghese, C.A. Grimes, Nano Lett. 6 (2006) 215–218.
[21] D. Kuang, J. Brillet, P. Chen, M. Takata, S. Uchida, H. Miura, K. Sumioka, S.M. Zakeeruddin, M. Grätzel, ACS Nano 2 (2008) 1113–1116.
[22] Y. Kondo, H. Yoshikawa, K. Awaga, M. Murayama, T. Mori, K. Sunada, S. Bandow, S. Iijima, Langmuir 24 (2008) 547–550.
[23] H.-J. Koo, Y.J. Kim, Y.H. Lee, W.I. Lee, K. Kim, N.-G. Park, Adv. Mater. 20 (2008) 195–199.
[24] D. Polpanich, P. Tangboriboonrat, A. Elaïssari, Colloid Polym. Sci. 284 (2005) 183–191.
[25] J.H. Park, K.J. Choi, J. Kim, Y.S. Kang, S.-S. Lee, J. Power Sources 173 (2007) 1029–1033.
[26] J.H. Park, J.-H. Yum, S.-Y. Kim, M.-S. Kang, Y.-G. Lee, S.-S. Lee, Y.S. Kang, J. Photochem. Photobiol. A: Chem. 194 (2008) 148–151.
[27] J.H. Park, K.J. Choi, S.W. Kang, Y.S. Kang, J. Kim, J. Power Sources 183 (2008) 812–816.

[28] S. Nakade, T. Kanzaki, Y. Wada, S. Yanagida, Langmuir 21 (2005) 10803–10807.
[29] K.-S. Ahn, M.-S. Kang, J.-K. Lee, B.-C. Shin, J.-W. Lee, Appl. Phys. Lett. 89 (2006) 013103.
[30] A. Imhof, Langmuir 17 (2001) 3579–3585.
[31] R.A. Caruso, A. Susha, F. Caruso, Chem. Mater. 13 (2001) 400–409.
[32] P.A. Lovell, M.S. El-Aasser (Eds.), Emulsion Polymerization and Emulsion Polymers, Wiley, New York, 1997.
[33] F. Ito, G. Ma, M. Nagai, S. Omi, Colloids Surf. A: Physicochem. Eng. Asp. 201 (2002) 131–142.
[34] P.J. Cameron, L.M. Peter, J. Phys. Chem. B 107 (2003) 14394–14400.